Comparison of Propylene/Ethylene Copolymers Prepared with Different Catalysts

C. H. Stephens,[1,*] B. C. Poon,[1,†] P. Ansems,[2] S. P. Chum,[2] A. Hiltner,[1] E. Baer[1]

[1]*Center for Applied Polymer Research, Department of Macromolecular Science and Engineering, Case Western Reserve University, Cleveland, Ohio 44106-7202*
[2]*Polyolefins and Elastomers R & D, The Dow Chemical Company, Freeport, Texas 77541*

Received 3 October 2005; accepted 21 November 2005
DOI 10.1002/app.23788
Published online in Wiley InterScience (www.interscience.wiley.com).

ABSTRACT: This study compared a series of experimental propylene/ethylene copolymers synthesized by a transition metal-based, postmetallocene catalyst (xP/E) with homogeneous propylene/ethylene copolymers synthesized by conventional metallocene catalysts (mP/E). The properties varied from thermoplastic to elastomeric over the broad composition range examined. Copolymers with up to 30 mol % ethylene were characterized by thermal analysis, density, atomic force microscopy, and stress–strain behavior. The xP/Es exhibited noticeably lower crystallinity than mP/Es for the same comonomer content. Correspondingly, an xP/E exhibited a lower melting point, lower glass transition temperature, lower modulus, and lower yield stress than an mP/E of the same comonomer content. The difference was magnified as the comonomer content increased. Homogeneous mP/Es exhibited space-filling spherulites with sharp boundaries and uniform lamellar texture. Increasing comonomer content served to decrease spherulite size until spherulitic entities were no longer discernable. In contrast, axialites, rather than spherulites, described the irregular morphological entities observed in xP/Es. The lamellar texture was heterogeneous in terms of lamellar density and organization. At higher comonomer content, embryonic axialites were dispersed among individual randomly arrayed lamellae. These features were characteristic of a copolymer with heterogeneous chain composition. J Appl Polym Sci 100: 1651–1658, 2006

Key words: propylene-ethylene copolymers; metallocene copolymers; elastomers; plastomers

INTRODUCTION

Polyethylene and polypropylene constitute the two most highly consumed thermoplastics in the world. Their growth can be increased by copolymerization to create new materials with novel and enhanced properties. Contemporary advances in catalyst technology allow random copolymerization of ethylene with large amounts of comonomer. New families of ethylene/octene (EO) and ethylene/styrene (ES) copolymers offer a wide range of properties from thermoplastic to elastomeric. Although the properties span a continuous spectrum with comonomer content, the wide range in properties makes it convenient to classify them into categories. This allows fundamental comparisons with other materials with similar properties as well as material differentiation for application purposes. The classification approach was successfully applied to homogeneous ethylene/octene copolymers,[1] and ethylene/styrene copolymers,[2] made by The Dow Chemical Company (Midland, MI), and to model ethylene/vinyl chloride copolymers.[3] Although all were ethylene copolymers, their classification enabled fundamental understanding of their similarities and differences.[4]

Metallocene polymerization of propylene has focused primarily on the wide variety of chain microstructures that can be synthesized in homopolymers. These include hybrids of isotactic, syndiotactic, and atactic structures and different patterns of chain irregularities.[5,6] However, it is also possible to synthesize homogeneous copolymers of propylene with large amounts of a higher α-olefin, and thereby extend the classification approach developed with ethylene copolymers to propylene/octene copolymers[7] and propylene/hexene copolymers.[8]

Metallocene-catalyzed copolymerization of propylene with ethylene has been of interest primarily for the preparation of ethylene/propylene (EPR-type) and ethylene/propylene/diene (EPDM-type) elastomers.[9] The Dow Chemical Company recently developed a new postmetallocene catalyst system that allows polymerization of propylene with ethylene over a broad range of compositions in an isotactic fashion and with high molecular weight.[10] These copolymers

Correspondence to: A. Hiltner (ahiltner@case.edu).
**Present address:* Carnegie Mellon University, Pittsburgh, Pennsylvania 15219.
†Present address: The Dow Chemical Company, Freeport, Texas 77541.
Contract grant sponsor: The Dow Chemical Company.

TABLE I
Characteristics of Propylene/Ethylene Polymers

Polymer designation	Comonomer content (mol %)	M_w (kg mol^{-1})	M_w/M_n
mP/E0.0	0.0	282	2.2
mP/E3.1	3.1	318	2.0
mP/EH.0	11.0	150	2.3
mP/E13.6	13.6	110	2.1
mP/E18.8	18.8	201	2.1
mP/E25.2	25.2	219	2.1
mP/E30.8	30.8	193	2.0
xP/E0.0	0.0	316	2.7
xP/E4.3	4.3	329	2.2
xP/E7.6	7.6	296	2.2
xP/E12.1	12.1	285	3.1
xP/E16.1	16.1	262	2.2
xP/E19.2	19.2	263	2.4

exhibit relatively narrow molecular weight distribution and unique chain microstructures. Comonomer distribution and stereo-defect type and concentration differentiate the new copolymers from those based on currently available Ziegler–Natta catalysts[11–14] and metallocene catalysts.[15,16] As a consequence of the unique chain microstructure, propylene/ethylene copolymers made with the new catalysts exhibit excellent physical and mechanical properties, such as high elasticity, high tensile strength, low haze, and high transparency.[10]

Initial studies of the structure–property relationships reveal that the new propylene/ethylene copolymers exhibit a wide spectrum of properties.[17] The present study compares the solid state structure and properties of experimental propylene/ethylene copolymers prepared by the new Dow catalyst (xP/E) with propylene/ethylene copolymers prepared by conventional metallocene catalysts (mP/E) over a wide composition range.

EXPERIMENTAL

Experimental polypropylene and propylene/ethylene copolymers prepared with a postmetallocene catalyst developed by Dow (xP/E) and with metallocene catalysts (mP/E) were supplied in pellet form by The Dow Chemical Company (Midland, MI). The polymers are described in Table I. They are designated by the type of catalyst and the ethylene content in mole percent.

Films 400 μm thick were compression molded from the pellets. The pellets were sandwiched between Mylar® sheets and preheated at 190°C for 5 min under minimal pressure, cycled from 0 to 10 MPa pressure for 1 min to remove air bubbles, held at 10 MPa for 4 min, and cooled to ambient temperature at ~15°C min^{-1} in the press. The compression-molded films were subsequently stored at ambient temperature for 7–12 days.

Density was measured according to ASTM D1505–85 using small pieces cut from the compression-molded films. An isopropanol–water gradient column with a density range of 0.8 to 1.0 g cm^{-3} was used. The reported density is the average of at least three specimens and has an error of less than 0.0005 g cm^{-3}. Crystallinity was calculated from density using $\rho_a = 0.853$ g cm^{-3} and $\rho_c = 0.936$ g cm^{-3}.[18]

Specimens weighing 5–10 mg were cut from compression-molded films for thermal analysis. Thermograms were obtained on a Perkin–Elmer (Boston, MA) Series 7 differential scanning calorimeter (DSC) from −60 to 190°C with a heating/cooling rate of 10°C min^{-1}. Weight percent crystallinity was calculated from the heat of melting using a value of 209 J g^{-1} for the heat of fusion (ΔH_0) of the polypropylene crystal.[19]

Specimens for atomic force microscopy (AFM) were prepared by melting ~40 mg of film in an uncovered pan under nitrogen in a Rheometrics (New Castle, DE) DSC. Specimens were held at 190°C for 5 min and slowly cooled at 3°C min^{-1}. The resulting film was microtomed at −75°C to expose the interior and etched for 30 min with a 2 : 1 : 0.07 sulfuric acid, *o*-phosphoric acid, potassium permanganate solution,[20] which removed surface marks caused by microtoming. After aging 1 day at ambient temperature, AFM experiments were conducted in air with a commercial scanning probe microscope Nanoscope IIIa from Digital Instruments (Santa Barbara, CA) operating in the tapping mode. Measurements were performed at ambient conditions using intermediate tapping conditions. Height and phase images were recorded simultaneously.

Dynamic mechanical thermal analysis (DMTA) of aged films was carried out with a Polymer Laboratories (Boston, MA) Dynamic Mechanical Thermal Analyzer. A rectangular specimen with dimensions of 17 × 7 mm^2 was cut from the compression-molded film and tested in dynamic tension with 1% strain at 1 Hz from −80 to 10°C below the melting temperature.

The stress–strain behavior in uniaxial tension was measured with ASTM D1708 microtensile specimens cut from the aged films. Specimens were stretched in an Instron (Canton, MA) Model 1122 testing machine at a rate of 100% min^{-1}. Engineering stress and strain were defined conventionally.

RESULTS AND DISCUSSION

Crystallinity

The heating thermograms of mP/E polymers obtained after cooling at a rate of 10°C min^{-1} are shown in Figure 1(a). As expected for homogeneous copolymers,[1–3] increasing comonomer content decreased the

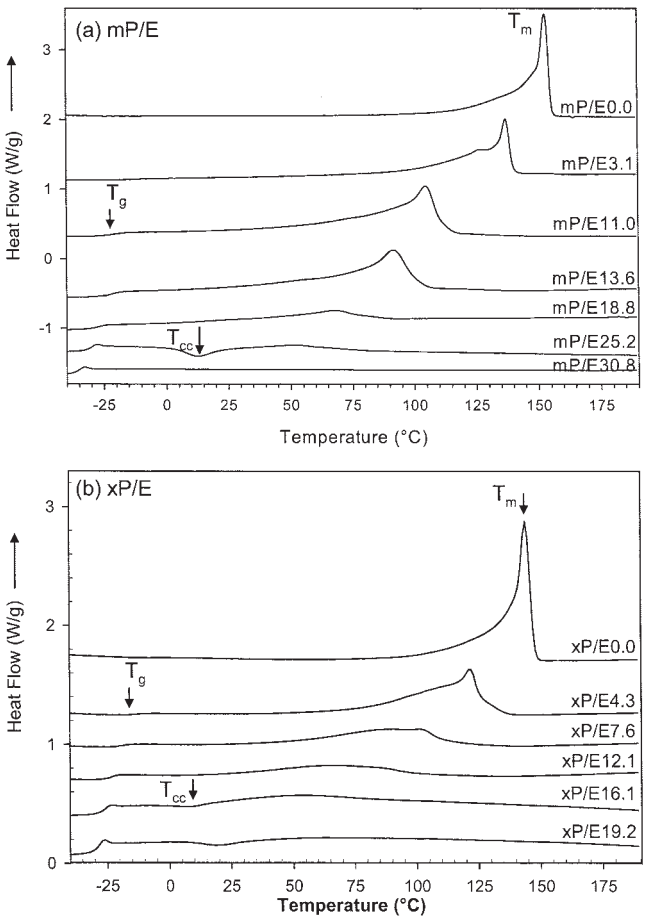

Figure 1 Heating thermograms obtained after cooling at 10°C m^{-1}: (a) mP/E and (b) xP/E.

peak melting temperature, broadened the melting endotherm somewhat, and lowered the heat of melting. With the exception of mP/E25.2, the mP/Es showed no indication of cold crystallization.

The heating thermograms of xP/E polymers are shown in Figure 1(b). The xP/E0.0 homopolymer had a sharp melting endotherm with peak melting temperature T_m of 145°C. As with the mP/Es, copolymerization with ethylene served to decrease the peak melting temperature, broaden the melting endotherm, and lower the heat of melting (Table II). However, for similar comonomer content, the xP/E exhibited a broader melting endotherm, lower peak melting temperature, and lower heat of melting than the mP/E. The melting endotherm of xP/E4.3 and xP/E7.6 was characterized by a relatively sharp peak superimposed on a broad melting region. The endotherm of the copolymers with higher ethylene content was so broad that it was difficult to define a peak melting temperature. The copolymers with even higher ethylene content, xP/E16.1 and xP/E19.2, did not completely crystallize during cooling, even at a fairly slow cooling rate of 10°C min^{-1}, as indicated by cold crystallization exotherms at T_{cc} of 10 and 20°C, respectively.

The homopolymers did not exhibit a glass transition inflection in thermograms due to the high crystallinity. However, thermograms of the copolymers showed a baseline inflection at lower temperatures that became stronger as the comonomer content increased. The glass transition inflection was more prominent in the thermograms of xP/Es than mP/Es. The glass transition temperature in the DSC thermograms decreased from −11°C for xP/E4.3 to −31°C for xP/E19.2. Overall, the thermal behavior of xP/Es suggested that they crystallized less readily with a less uniform crystal population than the mP/Es.

The effect of comonomer content on melting enthalpy is shown in Figure 2. For both mP/Es and xP/Es, crystallinity as reflected by ΔH_m decreased linearly with increasing comonomer content; however,

TABLE II
Properties of Propylene/Ethylene Polymers

Polymer	Density (g cm^{-3})	$X_{c,\rho}$ (wt %)	T_m (°C)	ΔH_m (J g^{-1})	X_c (wt %)	T_g (DSC) (°C)	T_g (DMTA) (°C)
mP/E0.0	0.9070	67	152	106	51	N/A	10
rnP/E3.1	0.9021	60	135	93	44	−12	5
mP/E11.0	0.8887	46	103	67	32	−19	−2
mP/E13.6	0.8851	41	92	55	26	−22	−6
mP/E18.8	0.8746	28	71	33	16	−27	−15
mP/E25.2	0.8625	12	56	15	7	−33	−17
rnP/E30.8	0.8550	3	49	3	1	−36	−26
xP/E0.0	0.9027	62	145	93	45	N/A	12
xP/E4.3	0.8945	52	121	76	36	−11	7
xP/E7.6	0.8882	45	98	62	30	−17	0
xP/E12.1	0.8801	35	84	47	22	−23	−6
xP/E16.1	0.8706	23	44	27	13	−25	−14
xP/E19.2	0.8617	11	44	12	6	−31	−20

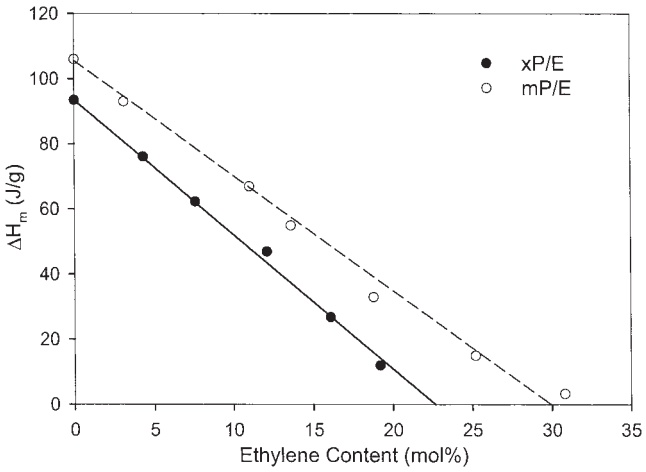

Figure 2 ΔH_m as a function of ethylene content for mP/E and xP/E.

crystallinity of xP/Es was consistently lower than crystallinity of mP/Es for a given comonomer content. As a result, about 30 mol % ethylene was required to achieve a completely amorphous mP/E copolymer, whereas, only about 23 mol % ethylene was projected to give a completely amorphous xP/E copolymer. This important difference suggested that xP/Es possessed a defect population and/or comonomer distribution that more effectively disrupted the crystallinity.

The heat of melting from DSC is often related to the composition of olefinic copolymers by the relationship

$$\Delta H_m = k(X_p)^n \tag{1}$$

where X_p is the mole percent propylene in the copolymer and the constant k is related to the heat of melting of the homopolymer.[21] Because eq. (1) is derived from probability arguments, n is expected to depend on the comonomer distribution and in the case of propylene copolymers, also on the defect type and distribution, which in turn are determined by the catalyst system and polymerization conditions. However, within a set of copolymers prepared by similar means, the application of eq. (1) is usually confirmed. The parameter n is sometimes interpreted as the minimum crystallizable sequence length.

The linear relationship between log ΔH_m and log X_p for metallocene-catalyzed copolymers of propylene and 1-octene (mP/O), a comonomer that is excluded from the polypropylene crystal, gave an n value of 10.[7] A similar value of 11 was reported for polypropylenes of different tacticity.[22] In contrast, xP/Es and mP/Es showed a weaker dependence of log ΔH_m on log X_p than that predicted for n of 10 (Fig. 3). Moreover, the relationship was not linear. An n value of about 5 was estimated for xP/Es and mP/Es with lower ethylene content. A value of n less than 10 indicated that ethylene units co-crystallized to some extent in the polypropylene unit cell. This was consistent with previous reports that described inclusion of ethylene units in the polypropylene crystal.[23,24] Results for xP/Es and mP/Es of higher ethylene content, i.e., those that crystallized slowly and exhibited cold crystallization, approached the line defined by mP/Os with n equal to 10 for comonomer exclusion. It can be speculated that as insertion of ethylene units became more frequent along the polymer chain, comonomer was not as easily accommodated in the polypropylene crystal.

Weight fraction crystallinity W_c from DSC taking ΔH_0 of 209 J g^{-1} was compared with weight fraction crystallinity from density measurements $W_{c,\rho}$ assuming a two-phase model with constant amorphous phase and crystalline phase densities

$$W_{c,\rho} = \frac{\rho_c}{\rho}\left(\frac{\rho-\rho_a}{\rho_c-\rho_a}\right)\times 100 \tag{2}$$

where ρ is the bulk density, ρ_a is the amorphous density, and ρ_c is the crystalline phase density. Using the generally accepted values of ρ_a and ρ_c for polypropylene of 0.853 and 0.936 g cm^{-3}, respectively,[18] crystallinity from density was consistently higher than crystallinity from DSC heat of melting W_c (Table II). Poor correlation between crystallinity from heat of melting and crystallinity from density was observed previously for polypropylene.[25] The assumption of constant amorphous phase density may not be appropriate for propylene copolymers. For measurements at ambient temperature, it may be necessary to consider an amorphous phase density that increases with the amount of crystallinity.[26]

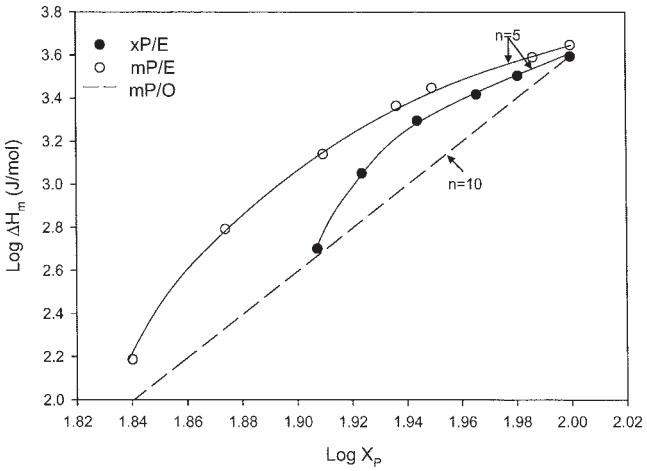

Figure 3 Logarithmic plot of DSC heat of melting *versus* propylene mole fraction for mP/E and xP/E compared with results for propylene/octene copolymers from Ref. 7.

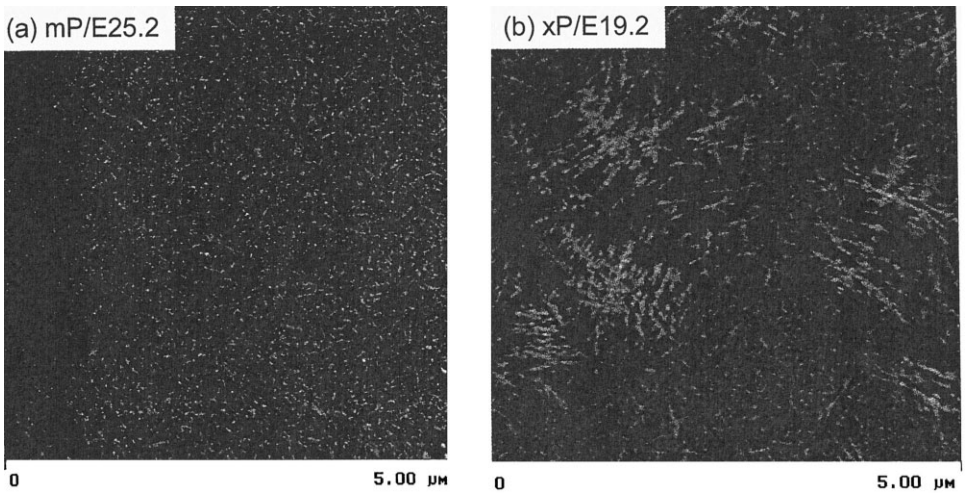

Figure 4 AFM phase images: (a) mP/E25.2 with 7% crystallinity and (b) xP/E19.2 with 6% crystallinity.

In comparing the crystalline morphology of the two families of copolymers, it was noted that mP/E copolymers with homogeneous chain composition exhibited space-filling spherulites with uniform lamellar texture. The main effects of increasing comonomer content were to decrease spherulite size until spherulitic entities were no longer discernable, and to decrease the overall lamellar density in the spherulite. In contrast, xP/E copolymers exhibited heterogeneous crystalline morphologies. Axialites more appropriately described the irregular morphological entities observed at lower resolution. Even when the axialites were space-filling, the lamellar texture was not homogeneous but appeared to vary in terms of lamellar density and organization. Increasing comonomer content decreased the lamellar density, however, the lamellar texture remained heterogeneous.

The main morphological differences between mP/Es and xP/Es are readily illustrated by comparing AFM images of copolymers with different comonomer content, but with about the same low level of crystallinity (Fig. 4). The morphology of mP/E25.2 with 7% crystallinity consisted of a homogeneous dispersion of short lamellae [Fig. 4(a)]. In contrast, the image of xP/E19.2 with 6% crystallinity showed embryonic axialites dispersed among individual randomly arrayed lamellae. The axialites consisted of long lamellar lathes with numerous overgrowths [Fig. 4(b)]. The morphology of xP/Es was characteristic of copolymers with heterogeneous chain composition.

Glass transition

The dynamic mechanical relaxation behavior of mP/Es and xP/Es is compared in Figure 5 with the temperature dependence of tan δ. The β-relaxation is identified as the glass transition. The peak temperature for mP/Es decreased from 10°C for mP/E0.0 to −15°C for mP/E18.8. Over a similar composition range, the peak temperature of xP/Es decreased from

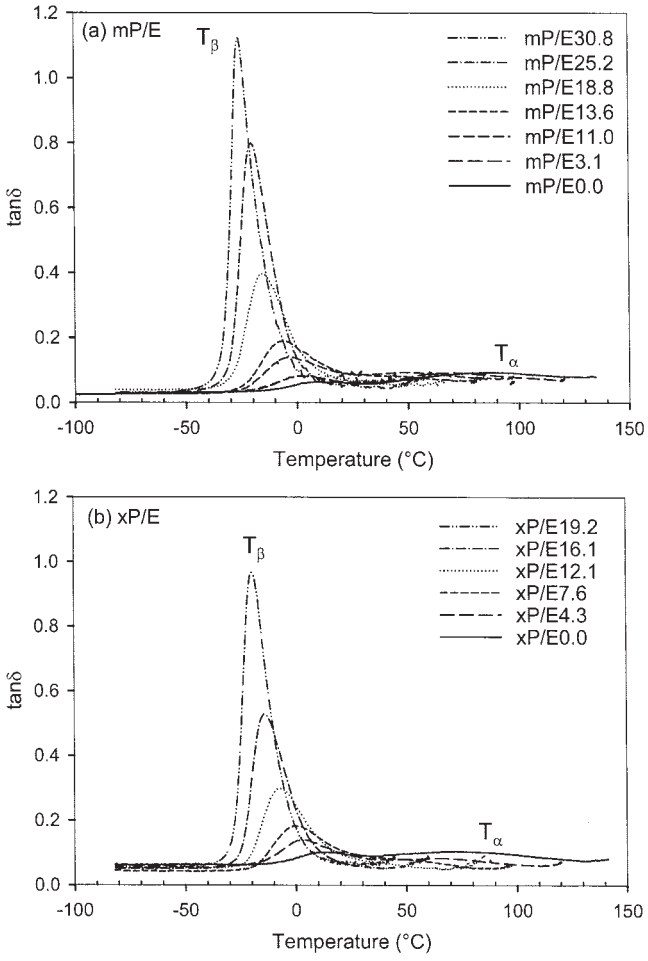

Figure 5 Effect of comonomer content on tan δ: (a) mP/E and (b) xP/E.

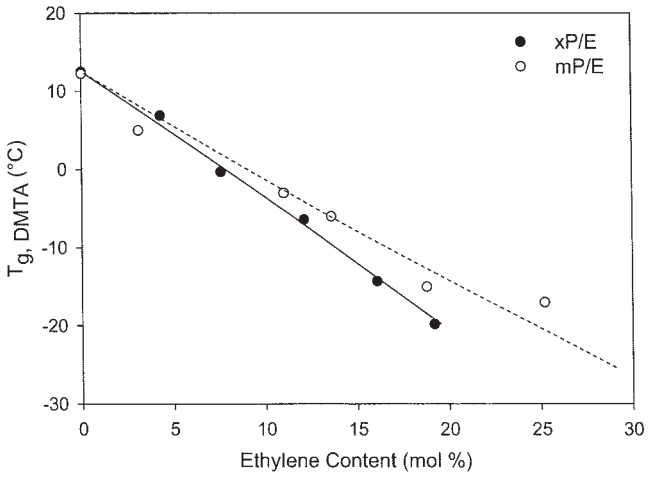

Figure 6 Glass transition temperature from tan δ as a function of comonomer content.

12°C for xP/E0.0 to −20°C for xP/E19.2. Increasing intensity of the tan δ peak with increasing comonomer content reflected an increase in the amount of amorphous phase. For copolymers of comparable ethylene content, the tan δ peak was stronger in the xP/E than in the mP/E due to lower crystallinity of the xP/E. The α-relaxation at about 75°C was observed for polymers of higher crystallinity. The α-relaxation represents a premelting phenomenon associated with increased mobility of chain segments in the crystal and in the interfacial region between the crystalline and amorphous phases.[27] It was difficult to discern the α-peak in copolymers with more than 14 mol % ethylene.

The effect of ethylene content on the glass transition temperature T_g taken as the peak temperature in the tan δ curves is plotted in Figure 6. The T_g decreased essentially linearly with comonomer content. The stronger dependence of T_g on comonomer content for xP/Es compared to mP/Es was consistent with lower crystallinity of xP/Es.

Mechanical properties

The effect of ethylene content on uniaxial stress–strain behavior is shown in Figure 7. The homopolymers had characteristics typical of a semicrystalline thermoplastic. Highly localized yielding coinciding with initiation of a sharp neck was followed by cold drawing as the neck propagated. The increase in engineering stress beginning at about 300% strain was associated with strain-hardening. At roughly 700% strain, the homopolymers fractured.

With increasing ethylene content, the modulus decreased, the yield stress decreased, the neck became more diffused, and the natural draw ratio decreased as indicated by the onset of strain-hardening at a lower engineering strain. Although the fracture strain did not vary significantly with comonomer content, the amount of recovery after fracture increased from almost no recovery of the homopolymer to almost complete recovery of the copolymer with highest ethylene content. These trends reflected decreasing crystallinity.

Although the stress–strain behavior changed continuously with comonomer content, the behavior of copolymers with lower ethylene content classified them as plastomers. These copolymers exhibited diffuse necking at a yield stress that was significantly lower than that of the homopolymer, and some cold-drawing followed by strain-hardening to fracture at high strain. Copolymers with higher ethylene content were identified as elastomers. They exhibited uniform deformation with low initial modulus, followed by gradually increasing stress to fracture at high strain and almost complete recovery after fracture.

Qualitatively, increasing comonomer content had the same effect on stress–strain properties of mP/Es and xP/Es. However, systematically lower modulus and yield stress of an xP/E compared to an mP/E of about the same ethylene content was consistent with the lower crystallinity of the xP/E. The difference between xP/Es and mP/Es was most dramatic in copolymers of higher ethylene content. Whereas, mP/E20.0 showed a broad yield maximum in the stress–strain curve and formation of a shallow neck, xP/E19.2 of similar ethylene content exhibited uniform deformation. The higher ethylene content of mP/E25.2 was required to achieve elastomeric behavior comparable with xP/E19.2.

The 2% secant modulus and the engineering yield stress were extracted from the stress–strain response (Fig. 8). The decreasing trend with ethylene content qualitatively matched the change in crystallinity. Thus, the mechanical properties of mP/Es decreased monotonically on the logarithmic scale and were systematically higher than the parameters obtained for xP/Es. The difference between xP/Es and mP/Es was magnified at higher ethylene content.

CONCLUSIONS

This study compared a series of experimental propylene/ethylene copolymers synthesized by a new postmetallocene catalyst (xP/E) with homogeneous propylene/ethylene copolymers synthesized by conventional metallocene catalysts (mP/E). Comonomer content affected mP/Es as expected for copolymers with random comonomer insertion and homogeneous chain composition. Despite some inclusion of ethylene units in the polypropylene crystal, the melting point, crystallinity, glass transition temperature, and mechanical properties decreased monotonically with the

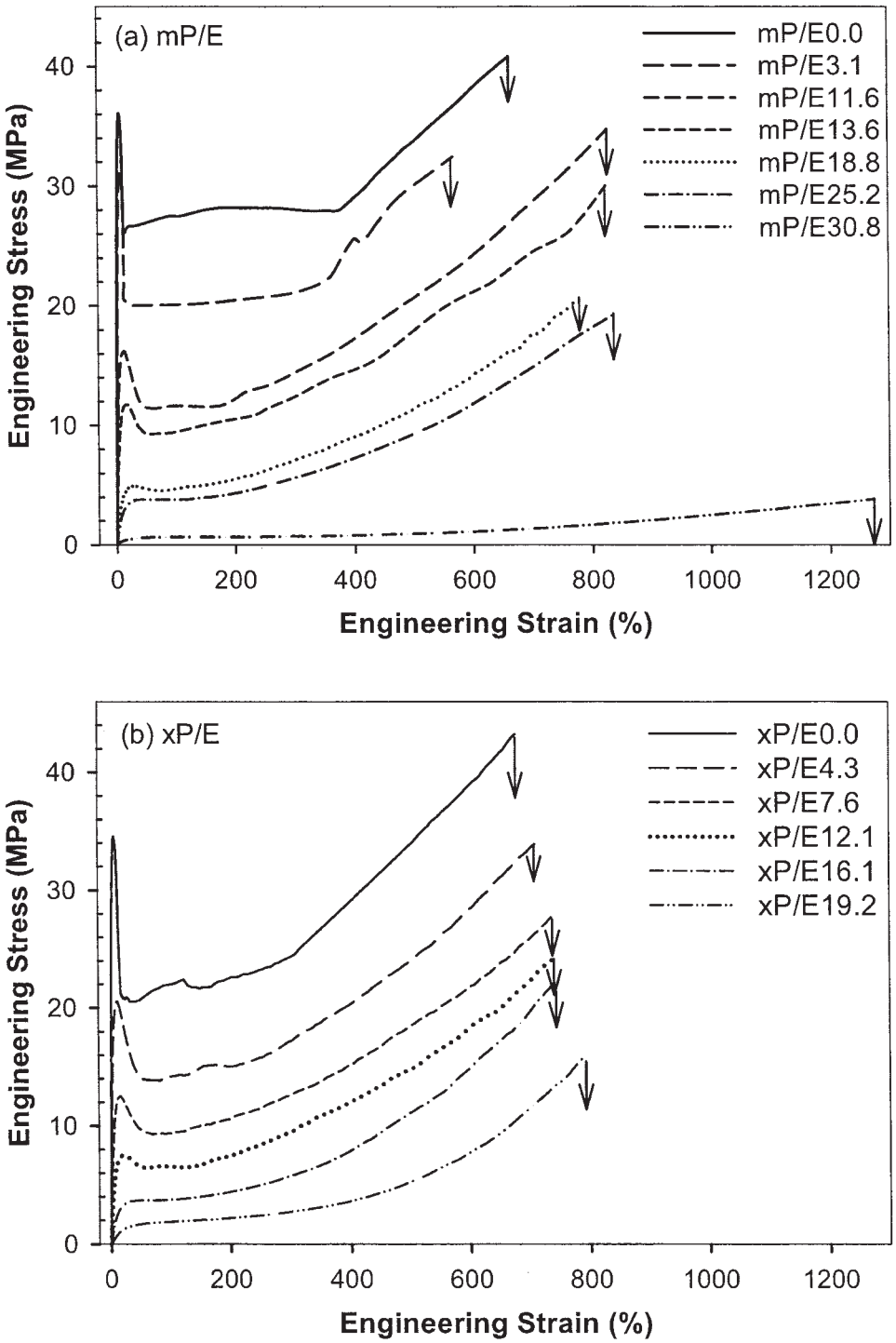

Figure 7 Engineering stress–strain curves: (a) mP/E and (b) xP/E.

comonomer content. The mP/Es crystallized as space-filling spherulites with uniform lamellar texture. The effect of increasing comonomer content was to decrease spherulite size until spherulitic entities were no longer discernable, and to decrease the overall lamellar density of the spherulite. The xP/Es exhibited somewhat lower crystallinity than mP/Es of the same comonomer content. This affected properties that directly related to crystallinity, such as modulus and yield stress. Axialites more appropriately described the irregular morphological entities of xP/Es. The lamellar texture was not homogeneous but appeared to vary in terms of lamellar density and organization. With increasing comonomer content, the lamellar texture remained heterogeneous with embryonic axialites dispersed among individual randomly arrayed lamel-

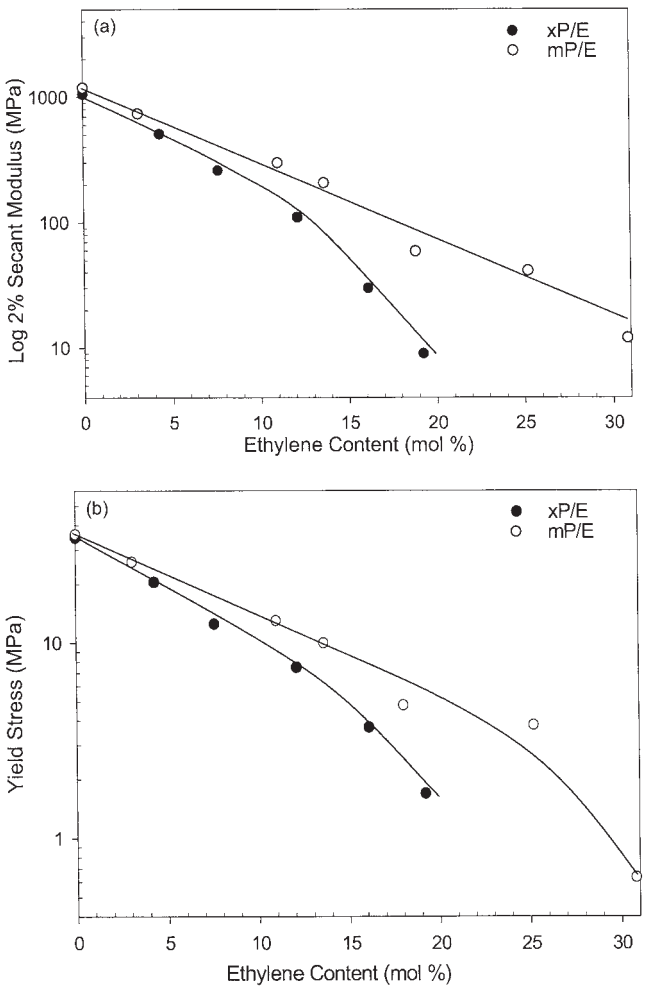

Figure 8 Mechanical properties as a function of comonomer content: (a) 2% secant modulus and (b) yield stress.

lae. These features were characteristic of a copolymer with heterogeneous chain composition.

The authors thank the Dow Chemical Company for providing the technical support.

References

1. Bensason, S.; Minick, J.; Moet, A.; Chum, S.; Hiltner, A.; Baer, E. J Polym Sci Part B: Polym Phys 1996, 34, 1301.
2. Chen, H.; Guest, M. J.; Chum, S.; Hiltner, A.; Baer, E. J Appl Polym Sci 1998, 70, 109.
3. Stephens, C. H.; Yang, H.; Islam, M.; Chum, S. P.; Rowan, S. J.; Hiltner, A.; Baer, E. J Polym Sci Part B: Polym Phys 2003, 41, 2062.
4. Chen, H. Y.; Chum, S. P.; Hiltner, A.; Baer, E. J Polym Sci Part B: Polym Phys 2001, 39, 1578.
5. Ewan, J. A.; In Metallocene-Based Polyolefins; Scheirs, J., Kaminsky, W., Eds.; Wiley: New York, 2000; Vol. 1, p 3.
6. Wiyatno, W.; Chen, Z.-R.; Liu, Y.; Waymouth, R. M.; Krukonis, V.; Brennan, K. Macromolecules 2004, 37, 701.
7. Poon, B.; Rogunova, M.; Chum, S. P.; Hiltner, A.; Baer, E. J Polym Sci Part B: Polym Phys 2004, 42, 4357.
8. Poon, B.; Rogunova, M.; Hiltner, A.; Baer, E.; Chum, S. P.; Galeski, A.; Piorkowskia, E. Macromolecules 2005, 38, 1232.
9. Galimberti, M.; Piemontesi, F.; Fusco, O. In Metallocene-Based Polyolefins; Scheirs, J., Kaminsky, W., Eds.; Wiley: New York, 2000; Vol. 1, p 309.
10. Swogger, K. W.; Poon, B.; Stephens, C. H.; Ansems, P.; Chum, S.; Hiltner, A.; Baer, E. In Proceedings of the Annual Technical Conference of Society of Plastics Engineers; Society of Plastics Engineers: Brookfield, CT, 2003; p 1768.
11. Busico, V.; Corradini, P.; DeRosa, C.; Di Benedetto, E. Eur Polym J 1985, 21, 239.
12. Zimmermann, H. J. J Macromol Sci Phys 1993, 32, 141.
13. Laihonen, S.; Gedde, U. W.; Werner, P.-E.; Westdahl, M.; Jääskeläinen, P.; Martinez-Salazar, J. Polymer 1997, 38, 371.
14. Avella, M.; Martuscelli, E.; Della Volpe, G.; Segre, A.; Rossi, E.; Simonazzi, T. Makromol Chem 1986, 187, 1927.
15. Fujiyama, M.; Inata, H. J Appl Polym Sci 2002, 85, 1851.
16. Alamo, R. G.; Blanco, J. A.; Agarwal, P. K.; Randall, J. C. Macromolecules 2003, 36, 1559.
17. Chum, S.; Stephens, C. H.; Poon, B.; Ansems, P.; Hiltner, A.; Baer, E. In Proceedings of the Annual Technical Conference of Society of Plastics Engineers; Society of Plastics Engineers: Brookfield, CT, 2003; p 1775.
18. Brandrup, J.; Immergut, E. H. Polymer Handbook, 3rd ed.; Wiley: New York, 1989.
19. Wunderlich, B. Macromolecular Physics; Academic Press: New York, 1980; Chapter 3, p 63.
20. Freedman, A. M.; Bassett, D. C.; Vaughan, A. S.; Olley, R. H. Polymer 1986, 27, 1163.
21. Burfield, D. R. Macromolecules 1987, 20, 3020.
22. Burfield, D. R.; Loi, P. S.; Doi, Y.; Mejzik, J. J Appl Polym Sci 1990, 41, 1095.
23. Alamo, R. G.; VanderHart, D. L.; Nyden, M. R.; Mandelkern, L. Macromolecules 2000, 33, 6094.
24. Hosoda, S.; Hori, H.; Yada, K.; Nakahara, S.; Tsuji, M. Polymer 2002, 43, 7451.
25. Isasi, J. R.; Mandelkern, L.; Galante, M. J.; Alamo, R. G. J Polym Sci Part B: Polym Phys 1999, 37, 323.
26. Wang, H. P.; Ansems, P.; Chum, S. P.; Hiltner, A.; Baer, E. Macromolecules, in press.
27. Passaglia, E.; Martin, G. M. J Res NBS A: Phys Chem 1964, 68, 519.